

Green infrastructures and their impact on resilience

Spatial interactions in centralized sewer systems

Mayra Rodriguez
CWS/AWMC
QUEX Institute
Exeter, UK
mr604@exeter.ac.uk

Guangtao Fu
CWS
University of Exeter
Exeter, UK
g.fu@exeter.ac.uk

David Butler
CWS
University of Exeter
Exeter, UK
d.butler@exeter.ac.uk

Abstract

Resilience in urban drainage infrastructure management has gained traction in the last few years, where systems need to adapt and recover from failure in face of deep uncertain threats. Green infrastructures, on-site nature-based stormwater strategies, are a promising concept that has proven to be effective in increasing the overall resilience performance in sewer systems. However, the improvement is not always significant or guaranteed. There is a lack of understanding of the local effects of these infrastructures and the spatial components of the impact on resilience in the network.

In this work, the spatial interactions between GI placement and improvements in the centralized sewer networks resilience were studied, whilst considering a wide range of design storms. Resilience is assessed using two metrics: flood volume and flood duration. The scenarios simulated were baseline scenarios with no green infrastructure for each rainfall (scenarios type 1) and a placement scheme using critical component analysis (scenarios type 2). The spatial interactions were analysed through three main points, the magnitude of the impact, the number of affected nodes and the location of the impact in the network. This analysis was applied in a case-study in the United Kingdom.

Regarding the magnitude of the impact, even though at a system level the impact is not high, at a node level the impact can be significant. Also, the impact is higher in shorter duration and lower return period storms. Regarding the number of affected nodes, most of the nodes remain unchanged. When all the scenarios are considered, there are as many nodes with an increase, as there are with a decrease in flooding volume and duration. Regarding the location of the impact, the nearest nodes to the outlet show the highest reduction in flood volume and flood duration. Subcatchments upstream the network and with highest areas seem to be the most impactful in the flood volume change. For flood duration, the subcatchments with smaller areas and generally in a middle region in the network cause the highest changes.

This study is a first approximation to understand spatial considerations regarding the impact on resilience based on different green infrastructure location in the network.

Permission to make digital or hard copies of part or all of this work for personal or classroom use is granted without fee provided that copies are not made or distributed for profit or commercial advantage and that copies bear this notice and the full citation on the first page. Copyrights for third-party components of this work must be honored. For all other uses, contact the owner/author(s).

ARIC'20, November 3–6, 2020, Seattle, WA, USA
© 2020 Association for Computing Machinery.
ACM ISBN 978-1-4503-8165-9/20/11...\$15.00
<https://doi.org/10.1145/3423455.3430302>

CCS CONCEPTS

• **Applied computing** ~Physical sciences and engineering
~Engineering • **Networks** ~Network performance evaluation
~Network performance analysis

KEYWORDS

green infrastructures, centralised sewer systems, resilience, urban flooding

ACM Reference format:

Mayra Rodriguez, Guangtao Fu and David Butler. 2020. Green infrastructures and their impact on resilience – Spatial interactions in centralized sewer systems. In *Proceedings of ACM ARIC 2020: 3rd ACM SIGSPATIAL International Workshop on Advances in Resilient and Intelligent Cities (ARIC'20)*. ACM, New York, NY, USA, 9 pages. <https://doi.org/10.1145/3423455.3430302>

1. Introduction

Urban drainage systems in high- and middle-income countries are generally provided through centralized networks with combined sewers [1,2]. General issues on traditional management restrict the ability to meet the current and future challenges of the sector, such as urbanisation, climate change, population growth and ageing infrastructure [3,4].

As an alternative to traditional urban stormwater management, green infrastructures (GI) are on-site ‘nature-based’ sustainable stormwater strategies that enable reversing hydrological and water quality impacts of urbanisation [5,6]. They have gained importance due to their multi-functionality, their flexibility and their potential in increasing resilience in urban drainage systems [5,7]. Previous research and applications of GI have proven these infrastructures to be effective, however, there are still various gaps in research and technical challenges [8,9]. This study specifically targets the gaps in, 1) the assessment of the impact of resilience in the sewer system considering local effects under a range of rainfall events, and 2) the spatial interactions between resilience improvements and GI placements in the network.

Improving the resilience of urban drainage infrastructure is a topic of interest and the integration of green infrastructures with the traditional urban drainage systems with this purpose are at heart of government policies and industry practices [9,10]. Sweetapple et al. [11] demonstrated a positive impact on the overall resilience performance in the system, although the improvement is not always significant or guaranteed. Using a cellular automata surface model, Wang et al. [12] proposed a

resilience metric for assessing flood resilience and the impact of adaptation measures on resilience in the system as a whole, and at a subcatchment level. These studies show the importance of resilience assessment in the implementation of green infrastructures, and how their impact is not always straightforward. However, they do not consider local effects and spatial considerations for the improvement of resilience based on GI location in the urban drainage system.

Determining the most appropriate strategy for the placement of green infrastructure, either in new developments or retrofitting in existing drainage systems, poses a challenging problem. This is due to their complexity, the uncertainty in their operation now and in the future (i.e. climate change, urbanisation and population growth), the lack of standardized performance assessment, and the unique characteristics of each drainage system [7,9,13,14,15]. Following an optimisation approach, Liu et al. [16] used a multi-criteria analysis for the support of GI scheme selection and Wang et al. [17] used an analytic hierarchy process module combined with iteration module for the optimal location of storage tanks. Based on biophysical factors and socio-demographic factors, Kuller et al. [18] proposed a planning support tool for spatial suitability of GI. This tool was later integrated by Bach et al. [19] in the UrbanBEATS model, which integrates stormwater management with urban planning to support the implementation of WSUD. In a simpler manner and focusing on local effects in the network, Zischg et al. [20] generated maps which allowed the identification of effective placements for green infrastructure. However, although the placement in the network was considered key in their studies, the implications on resilience and spatial interactions in the sewer systems were not reported.

This paper aims to gain understanding of the spatial interactions in the network in terms of resilience improvements by the implementation of GI. By this, it is expected to gain insight into the sensitivity to location of GI considering the effect of different return periods and duration storms.

2. Methodology

2.1 Simulation model

The modelling platform used in this study is the EPA Stormwater Management Model (SWMM), as it is a widely used model in the urban drainage system field that can simulate rainfall-runoff and contaminant transport. Primarily developed for urban areas, SWMM is a hydrological and hydraulic model that can be used for a single event and continuous simulation of runoff quantity and quality [21].

In this study, the kinematic wave theory is used for flow routing computations and the modified Horton method is used to simulate infiltration in pervious areas.

2.2 GI scenarios

Two main types of scenarios are studied: type 1) no green infrastructure, type 2) placement scheme using critical component analysis. These are explained below.

1. *Scenarios type 1* or baseline scenarios, correspond to the catchment before the installation of GI, where the catchment is simulated for its characterisation. These scenarios are used as a baseline to assess the impact of GI in the system.
2. *Scenarios type 2*, in a similar way to the critical component analysis described by Johansson & Hassel [22] and the sensitivity analysis used by Zischg et al. [20],

an exhaustive exploration of the system state is performed to estimate the consequences of green infrastructures in the sewer system. The idea behind this is to identify strategic locations that produce the largest or most relevant consequences in the network, allowing the identification of the spatial criticalities in terms of resilience improvement for the sewer system's function. For this, different scenarios evaluate the effect of a uniform green infrastructure with the same parameters, size and type at different locations in the catchment. The only factor changed is the location where the green infrastructure is placed. The parameters to characterize the GI used in all the scenarios, are presented in Table 1. The values used are typical values used in literature [12,21].

To understand the effect of different return periods and storm durations in the performance of the GI. Different design rainfall events are used for all the scenarios mentioned above.

Table 1: Summary of GI characteristics, based on [12,21]

Parameter	Layer	Value/Description
Type	-	Bio-retention Cell
Area	-	500 m ² – If the area of the subcatchment studied is less than 500 m ² , then the area of the GI is equal to the total area of the subcatchment.
Berm height	Surface	150 mm
Surface roughness	Surface	0.1 (Manning's n)
Thickness	Soil	1200 mm
		Soil Capillary suction 50 mm
Porosity	Soil	0.5 (volume fraction)
Field capacity	Soil	0.2 (volume fraction)
Wilting point	Soil	0.1 (volume fraction)
Conductivity	Soil	137 mm/h
Conductivity slope	Soil	12.5
Suction head	Soil	50 mm
Height	Storage	600 mm
		Void ratio: 0.2
		Seepage: 12.5
Void ratio	Storage	0.2
Seepage factor	Storage	12.5 mm/h

2.3 Resilience assessment

In this study, resilience is defined as “the degree to which the system minimises the level of service failure magnitude and duration over its design life when subject to exceptional conditions” [23]. The two main components of resilience are then, magnitude and duration. Two metrics are used to illustrate the dynamic of system performance are defined below:

1. *Failure magnitude*: it is represented as the total flood volume, which refers to the overflows from all the network nodes.
2. *Failure duration*: is the total duration of the flooding at the node, which is the time taken to from the occurrence of flooding to the recovery of normal performance.

These two indicators are commonly used in surface flooding and urban drainage system hydraulic performance [17], and they are used for the computation of the flood resilience index developed by Mugume et al. [24].

Each metric is computed for every node using SWMM and Python packages, pySWMM [25] and SWMM toolbox [26]. For the system, the flood magnitude is the summation of all the flood in all the nodes, while the flood duration is the mean of the flood durations of all the nodes.

To compare and contrast different scenarios, the change between the baseline scenarios (type 1) and the scenarios type 2 is calculated using Equations (1) and (2) for flood volume and flood duration respectively:

$$\%FVC = 100 \times \frac{TFV_{Scenario\ 2} - TFV_{Scenario\ 1}}{TFV_{Scenario\ 1}} \quad (1)$$

$$\%FDC = 100 \times \frac{TFD_{Scenario\ 2} - TFD_{Scenario\ 1}}{TFD_{Scenario\ 1}} \quad (2)$$

where %FVC refers to the percentage of flood volume change and %FDC is the percentage of flood duration change. In Equation (1), TFV is total flood volume, and in Equation (2) TFD is the total flood duration. These are applied at a system level and a node level. At a node level, to avoid errors due to neglectable flooding values, only the nodes with flooding volumes higher than 15 L are considered.

2.4 Spatial interactions

To understand the spatial interactions in the network of resilience improvement and the implementation of green infrastructures three main characteristics are studied based on the two metrics proposed: a. the magnitude of the impact, b. the number of affected nodes, and c. the location of impact in the network. These points are explained below.

- Magnitude of the impact:* a comparison of the impact of GI between the baseline scenario (type 1) and the results of the different placement scenarios (type 2) is performed.
- Affected nodes:* the number of nodes that have a difference in the flood volume and the flood duration is considered. This is a way to understand the extent of the impact of GI in the network. To account this, the percentage of the total of nodes affected with an increase, decrease and those who remain unchanged regarding the flood volume and flood duration are compared.
- Location:* this section looks at where in the network the impact of green infrastructure occurs. In SWMM, flooding occurs specifically in the nodes, meaning that flooding events are on or alongside the sewer network. For this reason, the network spatial analysis is used instead of planar spatial methods. When distances are considered, the shortest path distances are used instead of Euclidean distances [27]. For calculating the shortest-path distance, the origin is the outlet of the subcatchment where the green infrastructure was installed, and the end is the node that is being studied. The shortest-path distance is then, the sum of the pipes' lengths between the two nodes. It is assumed that there is no predetermined direction in the flow. For calculating the shortest-path distances, the Python package Networkx is used [28]. To compare different scenarios effectively, the normalized distance has been used, which is the shortest path distance between the node and the outlet of the subcatchment studied divided by the average of the shortest path distances of all the nodes to the outlet of the

subcatchment studied. In addition, the GI placements with highest impact in the network is discussed.

3. Case-study application

3.1 Study area

The case-study presented is a satellite town of Exeter, located in the South West of England. The watershed consists of 220 sub-catchments with a total area of 73.3 ha, serving a population of approximately 4000 inhabitants (Figure 1). The combined sewers consist of 487 conduit links and junction nodes, 3 storage tanks. The percentage of impervious area in the subcatchments is between 0% and 100%, and the elevation ranges between -0.9m and 17.2m. The parameterization was based on GIS data and recommended values from technical design guides, planning regulations and literature [2, 29,30,31].

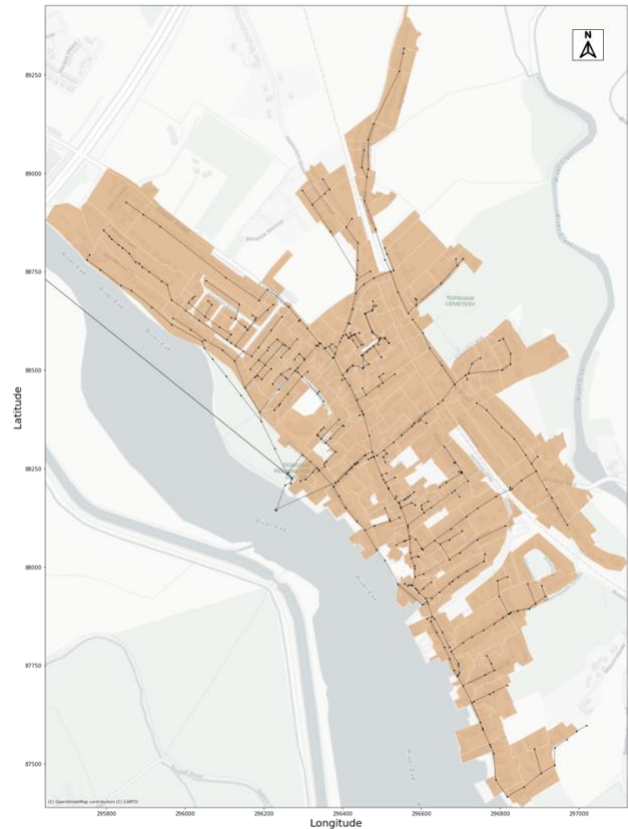


Figure 1: Layout of the case-study. Basemap by OpenStreetMap contributors [Public Domain], via OpenStreetMap Planet dump (<https://planet.openstreetmap.org>).

3.2 Rainfall events

Different desiring rainfall events with different durations and return periods were generated according to the Wallingford procedure [32]. The storm profile is built using the 50 % summer profile used in the FSR/FEH rainfall-runoff method, as recommended by the procedure [2, 33].

The return periods used were 2-, 10- and 100-year rainfall events, whereas the durations selected were 10, 30 and 60 minutes (Figure 2). In this paper, the storms are identified as My_D, where y refers to the return period and D is the storm duration.

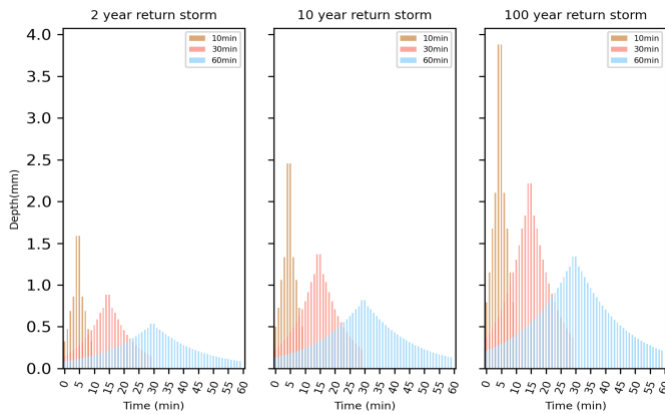


Figure 2: Design rainfalls used in the study

4. Results and discussion

4.1 Impact magnitude

4.1.1 System's magnitude impact.

Figure 3 shows the GI impacts at a system level, presented as the %TFV and %TFD in different storms.

Firstly, there is a great variation in the impact, which shows that there is a sensitivity to GI placement in the network. The mean of the differences between the baseline scenario and the type 2 scenarios, in each storm is negative, however, there are outliers showing the opposite effect. This means that there are locations that show an augmentation in flood volume and flood duration, which is the opposite effect expected by the application of GI. This will be further discussed in section 4.3.

Secondly, when comparing the effects on flood volume and flood duration, Figure 3 shows that in average, the effect in the flood volume is greater than in the flood duration. Although the variation of the flood volume is greater, the outliers shown in the flood duration are more prominent.

Finally, the inclusion of a GI one subcatchment at a time, only generates small effects at a system level, both for the flood volume and flood duration. This can be contrasted with Table 1, where even though effects at a system level are small, the effects at a node level are important. This is further discussed in the following subsection.

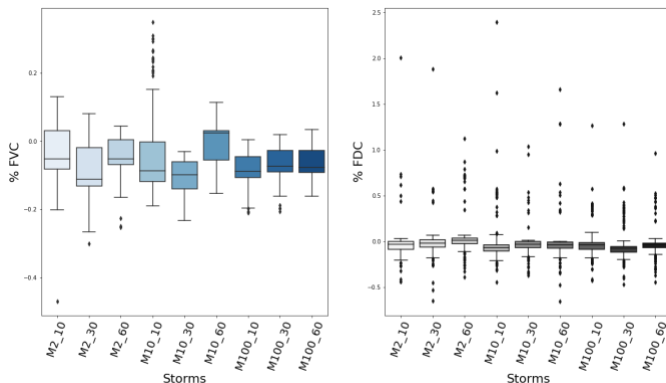


Figure 3: Variations at a system level in the %TFV and %TFD, based in the impact GI in the network.

4.1.2 Nodes' magnitude impacts.

Table 2 shows the variation in the impact of the implementation of GI at a node level, presented as the percentage difference between the scenarios type 2 and the baseline scenario (type 1).

In contrast to what happens at a system level, the effects of the implementation of GI are important at a node level. The change can be more than 85% and 55%, in flood volume and flood duration respectively. The mean of the change remains low due to the large number of unchanged nodes in all the scenarios considered. This is further discussed section 4.2.

Table 2: Ranges in the %FVD and %FDC, based on the impact of GI at a node level in the network.

Storm	%FVC				%FDC			
	Mean	SD	Min	Max	Mean	SD	Min	Max
M2_10	-0.17	1.66	-59.23	4.69	-0.04	0.96	-36	4.17
M2_30	-0.19	2.26	-79.3	6.99	-0.06	0.94	-42.86	3.57
M2_60	-0.15	1.96	-75.07	17.14	-0.02	0.97	-47.67	4.17
M10_10	-0.12	1.74	-67.45	11.03	-0.07	1	38.89	9.09
M10_30	-0.13	1.94	-79.91	9.92	-0.06	0.9	-49.12	6.38
M10_60	-0.18	2.13	-80.96	17.22	-0.12	1.13	-50	1.52
M100_10	-0.1	2.62	-80.38	257.23	-0.06	2.56	-57.14	433.33
M100_30	-0.06	3.09	-85.8	394.93	-0.17	3.04	-54.44	483.33
M100_60	-0.11	2.13	-86.53	4.3	-0.07	1.09	-55.32	2

4.1.3 Different Rainfalls.

Figure 3 and Table 2 show that when the mean in the change is considered, the GI impact is higher in shorter duration storms and smaller return period. However, generally, the range of values is higher for higher return periods storms.

4.2 Affected nodes

4.2.1 Unchanged, with an increase and with a decrease in the %FVC and %FDC at a node level.

Figure 4 shows the variation in the proportion of nodes that are affected by the implementation of the GI in scenarios type 2, differentiating rainfall events.

Most of the nodes remain unchanged, which as mentioned before, demonstrates that the implementation of the GI does not cause a general impact in the network, but it is restricted to some nodes in the network.

There are as many nodes with a decrease in flood volume and duration, as there are with an increase when considered all scenarios simulated. This does not consider the magnitude, but it is interesting to consider that even though the implementation of GI has a positive impact in certain areas of the network, this might generate a decrease in the performance in other areas. This is an important aspect to consider when choosing the right location of GI.

As the duration of the storms increases, there is an increase in the number of affected nodes. This is accentuated as the return period of the storm increases.

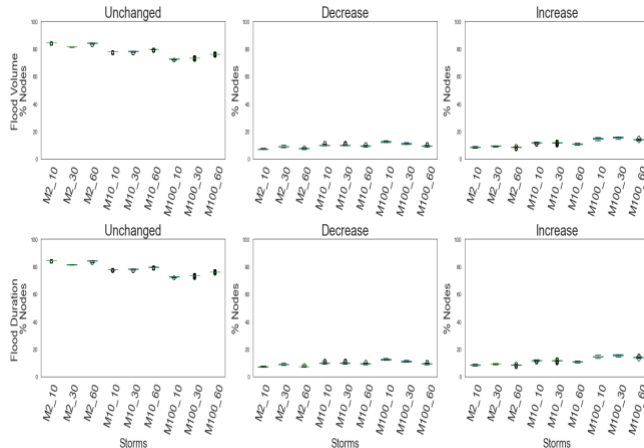


Figure 4: Affected nodes: unchanged, with a decrease and with an increase in the %FVC and %FDC, considering all the scenarios type 2 and design storms.

4.2.2 Affected nodes at different rainfalls.

When considering the kernel distribution estimation (KDE) plot (a non-parametric way to estimate the probability density function) and the rug plot (where each vertical line indicates an observation) for the difference flood volume between scenarios type 2 and the baselines (scenario type 1), it is noted that for different storm periods there is a similar pattern as the storm duration changes (Figure 5). As the duration of the storm increases, there is an increase in the nodes that have a higher flood volume change. This means that shorter storms tend to have more nodes affected, but with lower volume decrease/increase. A similar pattern is observed for difference in flood duration.

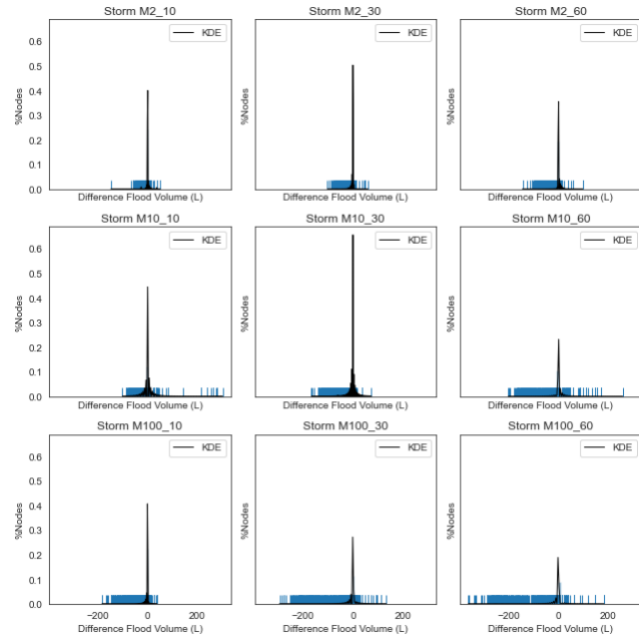


Figure 5: Distribution of affected nodes considering flood volume (L).

4.3 Location

4.3.1 Distance vs. magnitude impact.

Figure 6 presents the heatmaps showing the magnitude of %FVC and the normalized distance considering each node (y axis) and scenario type 2, where the GI were implemented one subcatchment (x axis). This means that each pixel in the plot corresponds to the value of %FVC or normalized distance for each node at each scenario type 2.

When comparing the two heatmaps, it can be seen that there is a clear relationship between %FVC and the normalized distance. The nodes nearer to the outlet where the GI has been implemented are the nodes where a change in the flood volume is considerable. A similar phenomenon is seen in all storms considered in the study, as well as when considering %FDC.

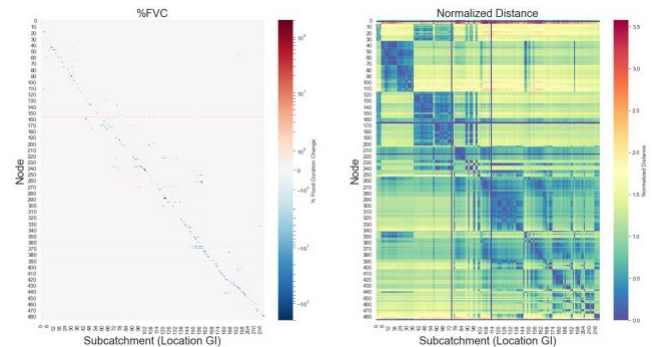


Figure 6: Heatmaps generated from the %FVC results of storm M100_60 (left) and normalized distance (right).

4.3.2. Distance distribution & magnitude impact.

Figure 7 shows the kernel distribution estimation plot, which allows seeing the bivariate distribution of the %FVC versus the normalized distance. It can be seen that medium impacts due to the implementation GI which cause a decrease in the flooding volume are concentrated in nodes which are nearest to the outlet of the subcatchment where the GI was implemented. However, in higher distances, there is another conglomeration of points, which indicate the increase in flooding. This could indicate that the increase in flooding due to the implementation of GI tends to occur downstream in the network. A similar trend is observed when considering %FDC.

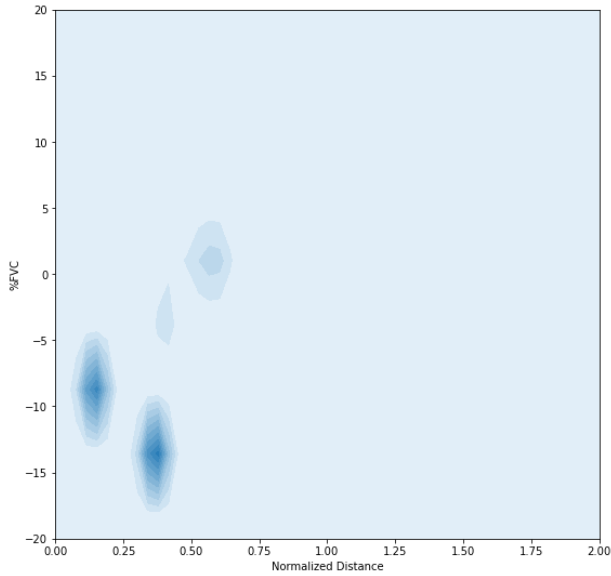


Figure 7: KDE plot %FVC vs. normalized distance, including all the scenarios type 2 and design storms.

4.3.3 Scenarios type 2 with the largest magnitude impact and their location.

Figure 8 shows the GI placements that generate the 10 highest flood volume reduction at node level for different storms. The 2-year return period storm differs mostly from the 10-year and 100-year return period storms. The subcatchments upstream in the network seem to be more impactful in higher return period and duration storms, whereas the subcatchments closer to downstream show higher decrease in the flood volume at lower return periods and shorter duration storms. There is greater coherence between different storms, as the same subcatchments are the most impactful in different storm. The subcatchments shown are in most cases the subcatchment with highest surfaces areas. Figure 9 showing the highest increase in volume location, show the opposite and these subcatchments are not the same in different storms.

When considering flood duration, the GI placements that cause the highest decrease are different than the subcatchments considered in flood volume (Figures 10 and 11).

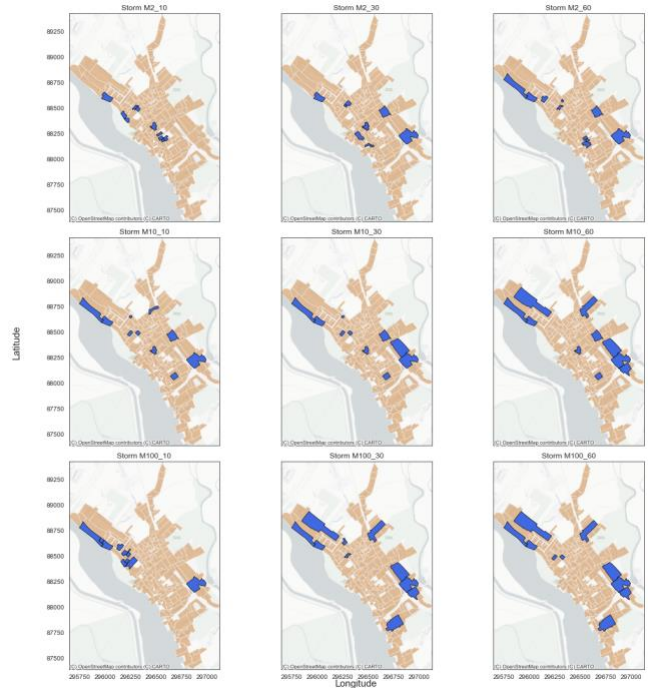


Figure 8: GI placement that cause highest flood volume reduction at node level for different storms. Basemaps by OpenStreetMap contributors [Public Domain], via OpenStreetMap Planet dump (<https://planet.openstreetmap.org>).

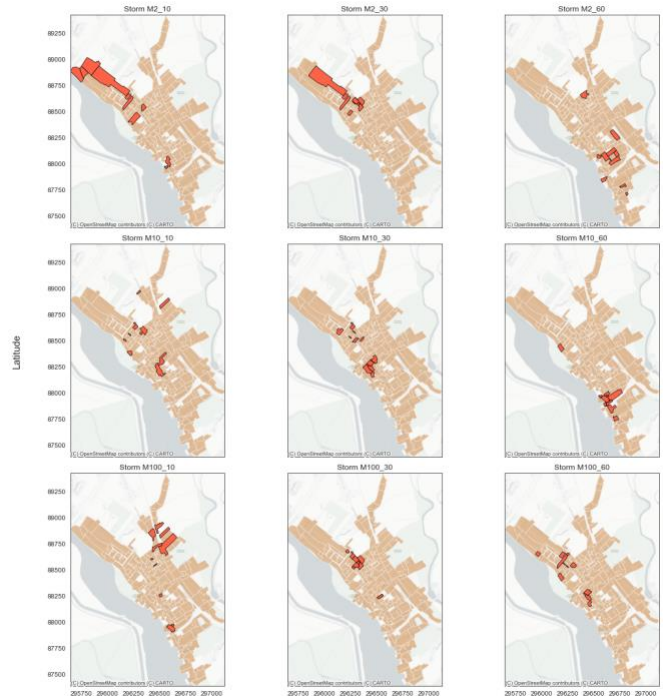


Figure 9: GI placement that cause highest flood volume increase at node level for different storms. Basemaps by OpenStreetMap contributors [Public Domain], via OpenStreetMap Planet dump (<https://planet.openstreetmap.org>).

The subcatchments where the GI placement cause the highest change in flood duration, contrary to the ones causing the highest decrease flood volume, are placed in a middle position in the network and have the smallest areas. However, there is more coherence between the subcatchments that have highest increase in flood duration and flood volume.

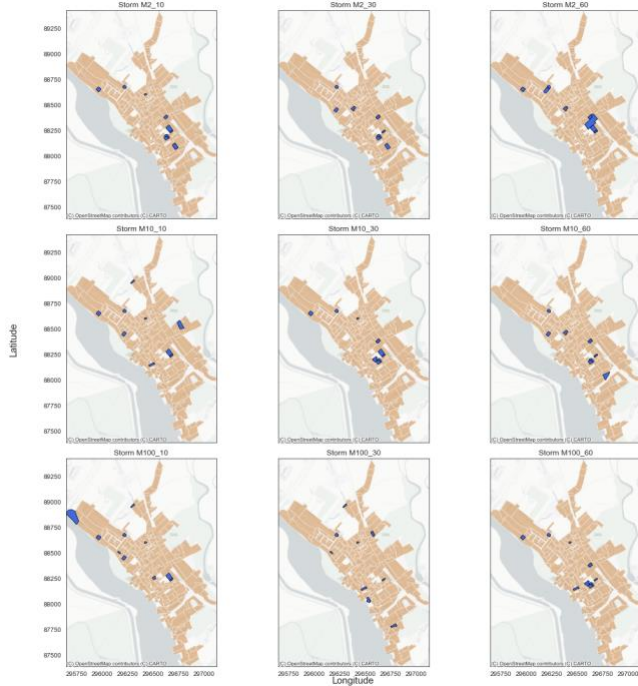


Figure 10: GI placement that cause highest flood duration decrease at node level for different storms. Basemaps by OpenStreetMap contributors [Public Domain], via OpenStreetMap Planet dump (<https://planet.openstreetmap.org>).

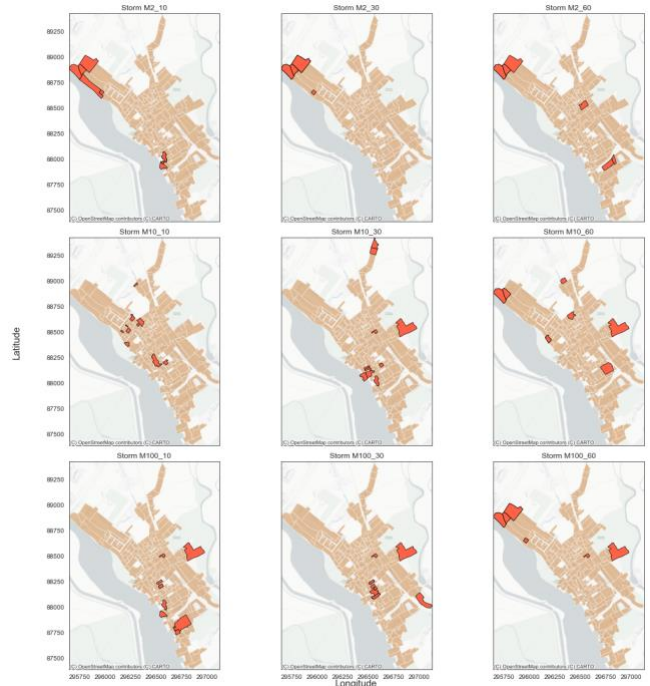


Figure 11: GI placement that cause highest flood duration increase at node level for different storms. Basemaps by OpenStreetMap contributors [Public Domain], via OpenStreetMap Planet dump (<https://planet.openstreetmap.org>).

4.4 Limitations & future research

The results presented cannot be generalized, due to the unique characteristics of each sewer system. However, this study represents an initial approach to spatial considerations of resilience regarding the network and green infrastructure placement. This approach can be used in other networks to enable a deeper understanding of spatial interactions between GI placements and resilience impacts in the network.

All the implemented GI are of the same type, parameters and area, so that the only variable changed in scenarios type 2 is location. However, GI include a wide diversity of strategies, and this should be considered in further studies to understand if alternative GI would bring different impacts on resilience.

Further steps in the implementation of this research will include spatial analysis tools, which will enable further spatial considerations of resilience. This would include in depth characterization of the urban form (i.e. imperviousness, land availability and slope), to have a further understanding of the interactions between these factors and the impacts of resilience at a node level. Furthermore, considerations of costs, land use and social aspects, as well as water quality indicators, could be integrated into the study to have further insight.

5. Conclusions

In this work, the impact of green infrastructures in centralized sewer systems and the spatial interactions in their impact on resilience has been studied.

Regarding the magnitude of the impact, the effect of GI in the sewer system seems to be localised and limited to a relatively small number of nodes. Some locations have significantly higher

impacts than others, and in some cases, there is an increase in flood volume and duration. The impact is higher in shorter duration and lower return period storms.

When considering nodal impact, a large proportion of nodes are not affected regarding flood volume and duration. In addition, when considering all the scenarios and storms, there are as many nodes with an increase in the metrics considered as there are with a decrease. This indicates that the placement of GI in respect to the network is critical to achieve an increase in performance (a decrease in flooding).

When considering location aspects, it can be seen that there is an important relationship between the most impacted nodes and their distance to the outlet of the subcatchment where the GI is placed. The nearest nodes to the outlet show the highest reduction in flood volume and flood duration.

Finally, when considering the metrics' highest increase and decrease for the different scenarios type 2, subcatchments upstream the network and with highest areas seem to be the most impactful in the flood volume change. This is different from the most impactful subcatchments in flood duration, where the subcatchments with smaller areas and generally in a middle region in the network cause the highest changes.

This study represents a first step towards the considerations of spatial interactions of resilience in the network and the GI implementation. Further research will consider other networks and will include relevant metrics, allowing a more holistic view on the topic.

Acknowledgments

M. Rodriguez was supported by the University of Exeter through a QUEX PhD scholarship – a joint initiative of the University of Exeter and The University of Queensland.

References

- [1] Hoffmann S., Feldmann U., Bach P.M., Binz C., Farrelly M., Frantzeskaki N., Hiessl H., Inauen J., Larsen T.A., Lienert J., Londong J., Lüthi C., Maurer M., Mitchell C., Morgenroth E., Nelson K.L., Scholten L., Truffer B., Udert K.M., 2020. A Research Agenda for the Future of Urban Water Management: Exploring the Potential of Nongrid, Small-Grid, and Hybrid Solutions. *Environmental Science and Technology*, 54(9), 5312–5322. DOI: 10.1021/acs.est.9b05222.
- [2] Butler D., Digman C., Makropoulos C., Davies J.W., 2018. *Urban drainage*. Boca Raton: Taylor & Francis, CRC Press.
- [3] Chocat B., Ashley R., Marsalek J., Matos M.R., Rauch W., Schilling W., Urbonas B., 2003. *Urban Drainage – Out of sight, out of mind? In Proceedings of 5th International Conference on Sustainable Techniques and Strategies in Urban Water Management (NOVATECH 2007)*. Novatech-Graie, Lyon, France.
- [4] Markard J., Raven R., Truffer B. Sustainability transitions: An emerging field of research and its prospects. *Research Policy* 2012, 41 (6), 955–967. DOI: <https://doi.org/10.1016/j.respol.2012.02.013>
- [5] Dhakal, K.P., Chevalier, L. R., 2017. Managing urban stormwater for urban sustainability: barriers and policy solutions for GI application. *Journal of Environmental Management*, 203 (1), 171-181. DOI: <https://doi.org/10.1016/j.jenvman.2017.07.065>
- [6] Li C., Peng C., Chiang P.C., Yanpeng C., Wang X., Yang Z., 2019. Mechanisms and applications of green infrastructure practices for stormwater control: A review. *Journal of Hydrology*. Elsevier, 568(2019), 626–637. DOI: 10.1016/j.jhydrol.2018.10.074.
- [7] Ahiablame, L.M., Engel, B.A., Chaubey, I., 2012. Effectiveness of LID practices: literature review and suggestions for future research. *Water, Air and Soil Pollution*, 223 (2012), 4253-4273. DOI: 10.1007/s11270-012-1189-2.
- [8] Browder, G., Ozment S., Rehberger Bescos I., Gartner T., Lange G.M., 2019. *Integrating Green and Gray: Creating Next Generation Infrastructure*. World Bank and World Resources Institute, Washington, DC, USA. URI: <http://hdl.handle.net/10986/31430>
- [9] Eckhart K., McPhee Z., Bolisetti T., 2017. Performance and implementation of low impact development – a review. *Science of the total environment*, 607-608 (2017), 413-432. DOI: 10.1016/j.scitotenv.2017.06.254
- [10] Ofwat, 2017. *Resilience in the round: building resilience for the future*. Ofwat, London, United Kingdom.
- [11] Sweetapple C., Gu F., Farmani R., Meng F., Ward S., Butler D., 2018. Attribute-based intervention development for increasing resilience of urban drainage systems. *Water Science and Technology*, 77(6), pp. 1757–1764. DOI: 10.2166/wst.2018.070.
- [12] Wang M., Wang Y., Gao X., Sweetapple C., 2019. Combination and placement of sustainable drainage system devices based on zero-one integer programming and schemes sampling. *Journal of Environmental Management*. Elsevier, 238(2019), 59–63. DOI: 10.1016/j.jenvman.2019.02.129.
- [13] Butler, D., Jowitt, P., Ashley, R., Blackwood, D., Davies, J., Oltean-Dumbrava, C., McIlkenny, G., Foxon, T., Gilmour, D., Smith, H., Cavill, S., Leach, M., Pearson, P., Gouda, H., Samson, W., Souter, N., Hendry, S., Moir, J., Bouchart, F., 2003. SWARD: decision support processes for the UK water industry. *Management of Environmental Quality: An international journal*, 14 (4), p. 444-459. DOI: <https://doi.org/10.1108/14777830310488676>
- [14] European Commission, 2013. *Green Infrastructure (GI) — Enhancing Europe's Natural Capital (2013/2663(RSP))*. European Commission, Brussels, Belgium.
- [15] Kuller M., Bach P.M., Ramirez-Lovering D., Deletic A., 2017. Framing water sensitive urban design as a part of the urban form: a critical review of tools for best planning practice. *Environmental modelling*, 96 (2016) 265-282. DOI: <https://doi.org/10.1016/j.envsoft.2017.07.003>
- [16] Liu Y., Cibir R., Bralts V.F., Chaubey I., Bowling L.C., Engel B.A., 2016. Optimal selection and placement of BMPs and LID practices with a rainfall-runoff model. *Environmental Modelling and Software*. Elsevier Ltd, 80, 281–296. DOI: 10.1016/j.envsoft.2016.03.005.
- [17] Wang M., Sun Y. and Sweetapple C., 2017. Optimization of storage tank locations in an urban stormwater drainage system using a two-stage approach. *Journal of Environmental Management*. Elsevier Ltd, 204, pp. 31–38. DOI: 10.1016/j.jenvman.2017.08.024.
- [18] Kuller M., Bach P.M., Roberts S., Browne D., Deletic A., 2019. A planning-support tool for spatial suitability assessment of green urban stormwater infrastructure. *Science of the Total Environment*. The Authors, 686, 856–868. DOI: 10.1016/j.scitotenv.2019.06.051.
- [19] Bach P. M., Kuller M., McCarthy D., Deletic A., 2020. A spatial planning-support system for generating decentralised urban stormwater management schemes. *Science of the Total Environment*. Elsevier B.V., 726, p. 138282. DOI:10.1016/j.scitotenv.2020.138282.
- [20] Zischg J., Zeisl P., Winkler D., Rauch W., Sitzenfrei R., 2018. On the sensitivity of geospatial low impact development locations to the centralized sewer network. *Water Science and Technology*, 77(7), 1851–1860. DOI: 10.2166/wst.2018.060.
- [21] Rossman L.A., 2015. *Storm Water Management Model User's Manual Version 5.1*. National Risk Management Research Laboratory, Office of Research and Development, US Environmental Protection Agency, Washington, DC, USA.
- [22] Johansson, J., Hassel, H., 2012. Modelling, simulation and vulnerability analysis of interdependent technical infrastructures. In:

- Hokstad, P., Utne, I.B., Vatn, J. (Eds.), Risk and Interdependencies in Critical Infrastructures - a Guideline for Analysis. Springer, London Heidelberg New York Dordrecht. DOI: 10.1007/978-1-4471-4661-2
- [23] Butler D., Ward S., Sweetapple C., Astaraie-Imani M., Diao K., Farmani R. & Fu G. 2016 Reliable, resilient and sustainable water management: the Safe & SuRe approach. Global Challenges. DOI:10.1002/gch2.1010
- [24] Mugume S. N., Gomez, D.E., Fu G., Farmani R., Butler D., 2015. A global analysis approach for investigating structural resilience in urban drainage systems. Water Research. Elsevier Ltd, 81, pp. 15–26. DOI: 10.1016/j.watres.2015.05.030.
- [25] McDonnell B. E., Ratliff K.M., Tryby M. E., Wu J.J.X., Mullanpudi A., 2020. PySWMM: The Python Interface to Stormwater Management Model (SWMM). Journal of Open Source Software, 5(52), 2292. DOI: <https://doi.org/10.21105/joss.02292>
- [26] Cera T., 2013. SWMM Toolbox – Overview (2013). Retrieved 27 August 2020 from <https://timcera.bitbucket.io/swmmtoolbox/docsrc/readme.html>
- [27] Okabe A., Sugihara K., 2012. Spatial Analysis along Networks – Statistical and computational methods. John Wiley & Sons, Chichester, United Kingdom.
- [28] Hagberg A.A., Schult D.A. and Swart P.J., 2008. Exploring network structure, dynamics, and function using NetworkX. In *Proceedings of the 7th Python in Science Conference (SciPy2008)*. Gael Varoquaux, Travis Vaught, and Jarrod Millman (Eds), Pasadena, CA, USA.
- [29] Woods Ballard B., Wilson S., Udale-Clarke H., Illman S., Scott T., Ashley R., Kellagher R., 2015. The Suds Manual (C753). CIRIA, London, United Kingdom.
- [30] Rossman L.A., Huber W.C., 2016. Storm Water Management Model Reference Manual III – Water Quality. National Risk Management Research Laboratory, Office of Research and Development, US Environmental Protection Agency, Washington, DC, USA.
- [31] OpenStreetMap contributors, 2015. Planet dump – Exeter, Devon, United Kingdom. Retrieved 27 August 2020 from <https://planet.openstreetmap.org>
- [32] DoE/NWC. 1981. Design and Analysis of Urban Storm Drainage. The Wallingford Procedure. Volume 1: Principles, Methods and Practice, Department of the Environment, Standing Technical Committee Report No. 28. Department of the Environment, London, United Kingdom.
- [33] Rodding Kjeldsen T., 2007. Flood Estimation Handbook – Supplementary Report No.1. Centre for Ecology & Hydrology, Wallingford, United Kingdom.